

**Title:** A New High-Pressure Optical Membrane Module for Direct Observation of Seawater RO Membrane Fouling and Cleaning

**Journal:** Journal of Membrane Science

**Authors:** Xiaofei Huang, Gregory R. Guillen, Eric M.V. Hoek

**Corresponding author:** Eric M.V. Hoek

**Institute:**

University of California, Los Angeles

**The original and creativity of paper:** They developed a high-pressure optical membrane module to enable direct observation of bacterial deposition on to membrane surface under seawater reverse osmosis desalination. This new novel

**Summary:**

The paper introduces new technique to visualize as well as diagnosis real-time membrane fouling. The historical of this instrument is start from microfiltration up to low-pressure reverse osmosis. Moreover, they developed quantitative methods and models to investigate physic-chemical mechanisms governing deposition and removal of colloidal particles and bacteria. The device can be applied into two categories: (1) fouling phenomena in situ quantification for lab-scale study and (2) employing on-line ex situ fouling and scaling detectors. In this study, they present the application of the device as a prototype high-pressure optical membrane module and demonstrate its abilities by estimating bacterial deposition onto seawater RO membrane at different permeate fluxes both with and without plastic feed spacers. The schematic diagram of optical membrane module was showed in Fig. 1.

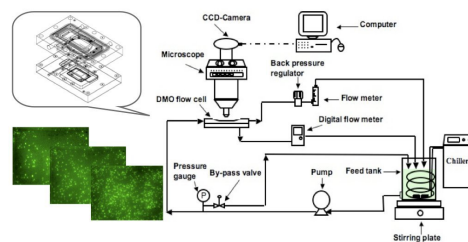


Fig. 1 Schematic diagram of optical membrane module integrated with pressure, flow and microscopic observation components.

The membrane module is a two pieces of 316 stainless steel. The top plate which provide feed and concentrate ports, the optical window, and the cross-flow channel. The bottom plate containing the permeate channel and port as shown in Fig 2.

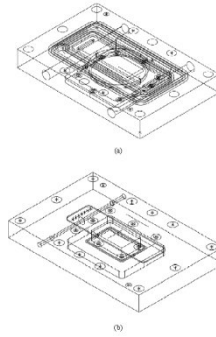


Fig. 2 Illustrations of for high-pressure optical membrane module including: (upper) top plate and (bottom) bottom plate.

A flat sheet membrane is sandwiched between these two plates with active side facing towards the top plate. The plates are bolted together by screws along the edges. The optical window material is a cylindrical piece of sapphire with 50.8 mm in diameter and 3.175 mm in thickness. A recession was created under the window region then fluid channel was tapered in the leading and ending region of the window to smooth the flow (Fig. 3).

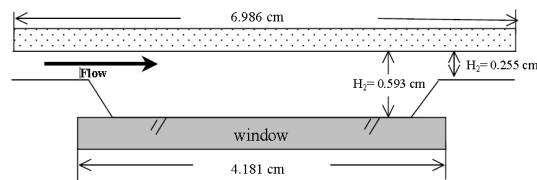


Fig. 3 Illustration of cross-flow channel geometry and dimensions.

The flow channel was designed to be 69.86 mm long, 25 mm wide, and 2.55 mm with the channel height. The window pocket window was 5.93 mm in height.

The velocity profiles is simulated and illustrated in Fig. 4. Fig. 4 illustrated that velocity reduced as the feed passed through the deeper viewer region. While the axial flow velocity distribution became highly irregular towards the tapered region on the outlet side. Moreover, stagnant zone was observed for both inlet and outlet channel at the viewing window. Based on this design, the device can only simulate low Reynold number cross-flow when feed spacer presence. For spacerless, more reasonable cross-flow hydrodynamic conditions can be simulated.

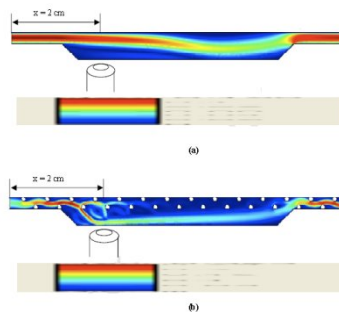


Fig. 4 Illustration of fluid flow patterns for inlet velocity of 8 cm/s (a) without a feed spacer and (b) with a feed spacer. Flow direction is from left to right. The microscope objective viewed the membrane surface at the location depicted.

Figure 5 shows the direct observation of bacterial deposition when feed spacer was absence. Fluorescent images were capture at the same spot at 5, 10, 15, and 20 min. Bacteria cells deposited evenly across both membrane surfaces were clearly viewed through the CCD camera which could provided an adequate image.

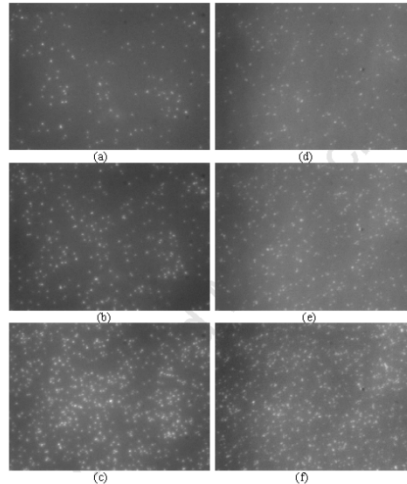


Fig. 5 Acquired microscope images of (a, b, c) SWC4+ and (d, e, f) SW30HR membranes at a fixed location. Images acquired at exposure times of (a, d) 5 min, (b, e) 10 min, and (c, f) 20 min with  $10^9$  cells/ml *H. pacifica* cells were dispersed in 32 g/l synthetic sea salt at pH adjusted to 6 by HCl addition, cross-flow Reynolds number of 534, and permeate velocity of  $7.2 \mu\text{m/s}$ .

Since in the real system, feed spacer was present. Fig. 7 shows microscopic images were taken at specific location around spacer. Because of the small viewing area of microscope, it is not easy to obtain across multiple spacer repeating units even at the lowest magnification. However, the researchers created a conceptual illustration from a mosaic of the deposition patterns microscopically observed within one repeating spacer mesh unit. Fig. 8 shows that bacteria cells accumulated more intensely between the spacer meshes. This refer that feed spacers may influence initial bacterial adhesion and colonization onto membrane surface. Interestingly, bacteria accumulated more readily on the backside of spacer filaments in the rear stagnant zone. On the other hand, less deposition was detected at the front of spacer filaments. The mentioned pattern agrees with the simulation result as showed in Fig 4.

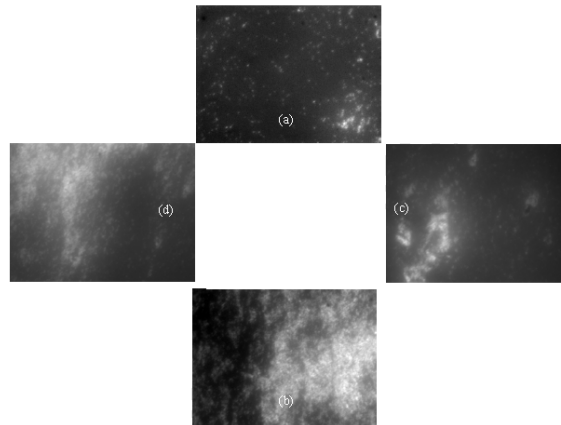


Fig. 7 Microscopic images of bacteria deposits on SWC4+ membrane surface at locations within a single repeating cell of the feed spacer: (a) front side of spacer filament facing towards the flow direction; (b) back side of spacer filament facing opposite to the flow direction; (c) right side of spacer filament; (d) left side of spacer filament. Images were captured after 30 min of operation with permeate velocity of  $7.2 \text{ m/s}$  and  $Re = 534$  in  $32 \text{ g/l}$  synthetic sea salt at  $pH = 6$ .

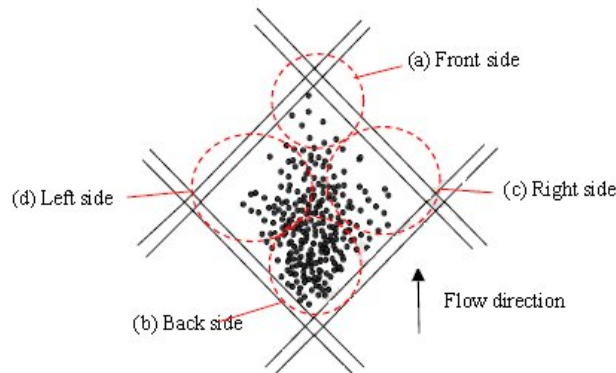


Fig. 8 Conceptual illustration of bacterial deposition pattern on SWC4+ membrane with feed spacer present in the cross-flow channel as seen through microscope eyepiece.

However, this research requires generalizations to confirm the behavior of the deposition pattern in any real spiral wound element.

**Application & further study:** This discovery can be include future study such as use it for examination RO membrane material under different operating condition, optimization of membrane cleaning, and use it as an ex situ fouling detector in a full scale seawater desalination plant.

By Monruedee Moonkhum  
Email: moon@gist.ac.kr